Ocean Monitoring Framework based on Compressive Sensing using Acoustic Sensor Networks

Ocean Monitoring Framework based on Compressive Sensing using Acoustic Sensor Networks

Rahul Mourya*[1], Wael Saafin[2], Mauro Dragone, Yvan Petillot
Institute of Sensors, Signals, and Systems
Heirot-Watt University Edinburgh, Scotland, UK
R.mourya@hw.ac.uk, W.saafin@hw.ac.uk, M.dragone@hw.ac.uk, Y.R.Petillot@hw.ac.uk

***Abstract*—This paper presents a framework for spatio-temporal monitoring of ocean environment using large-scale underwater acoustic sensor networks (UWASNs). Our goal is to exploit low-cost, battery-operated technology for acoustic communication to enable long-term, mass deployment of UWASNs for a wide range of monitoring applications in need of high spatio-temporal sampling rate and near real-time data delivery. Inspired by theory of compressive sensing (CS), the framework supports opportunistic random deployment of sensor nodes and relies on random channel access to harvest their data and construct spatio-temporal fields of the underlying sensed phenomena. In order to save bandwidth and energy, we consider a positioning scheme in which the sensor nodes remain silent and just listen for beacon signals from few reference nodes to localize themselves. After this initial localization phase, the sensing process begins. At regular intervals (frames), a set of random sensors sample their transducers and independently try to transmit their measurements to a fusion center (FC) for CS-based field reconstruction. Due to this random access of the acoustic channel, some of the packets may collide at the FC, wasting both energy and bandwidth. For slowly varying fields, consecutive frames have high correlations. We exploit this information during the field reconstruction, and show by simulation results that the number of sensors participating in each frame can be reduced drastically. This decreases the number of collisions at the FC, thus saving energy and prolonging the life-time of the network.**

***Index Terms*—Acoustic sensor networks, silent localization, random access, compressive sensing, convex optimization**

I. Introduction

Underwater acoustic sensor networks are widely becoming essential enablers for a wide range of applications such remote monitoring of ocean environments, marine biodiversity, anticipating natural disasters, underwater assets management, defense and homeland security, to name a few. Often, these require long-term deployment of sensor networks. Each sensor node in these networks is typically consists of a modem, some sensor modules, a computational unit for signal processing and network protocols, and a power supply. Acoustic communication is often the physical layer technology of choice for underwater wireless networking, since acoustic waves can travel long ranges (up to kilometers) while radio and optical waves die within few meters. However, unlike the terrestrial radio and optical channels, the underwater acoustic channel is constrained by three factors: limited and distance-dependent bandwidth, time-varying multi-path propagation, and low speed of sound [1]–[3]. Moreover, acoustic modems are typically limited to half-duplex operation. On top of that, supplying power to the underwater sensor nodes for long-term deployment is also a major concern. All these constraints pose a significant challenge for developing UWASNs and its protocols [4]–[6].

In this paper, we propose a framework for spatio-temporal monitoring of underwater physical phenomenon by measuring physical parameters such as temperature, pressure, salinity, oxygen level, etc, using UWASNs. With the recent advances in technologies, the acoustic modem, sensors and computing units are getting cheaper, reliable and power efficient, thus the UWASNs are becoming more realizable. However, the channel access is still one of the biggest obstacles due low bandwidth and long propagation delay. There are two main categories of multiple-access protocols that enable to share a channel among multiple communicating nodes: deterministic and random access. Deterministic access protocols share the channel in several ways (e.g. time-division, frequency-division, code-division) and avoid collision between the data packets. These protocols are suitable for applications that need a steady flow of information. In random access protocols, the nodes transmit their packets whenever they have new data without worrying about collisions. These protocols are good for applications that has very low-traffic and bursty information here and there. Several improvements on the standard multiple access protocols have been proposed in literature; see [4]–[6] and references within for detailed comparisons. Time division multiple access (TDMA) is one of the simplest deterministic protocols, but typically requires centralized clock synchronization among the nodes. Authors in [6] proposed a centralized clock synchronization free TDMA, which is a significant improvement over standard TDMA. Code division multiple access (CDMA) can outperform TDMA in many aspects: robustness to frequency-selective fading, compensation for the effect of multipath by exploiting Rake filters at the receiver, and enabling receivers to distinguish among signals simultaneously transmitted by multiple devices. Thus, it can be a promising physical and MAC layer technique for underwater communication. However, because of its high-computational

* Corresponding author
[1] is supported by EPSRC grant EP/P017975/1 for USMART project.
[2] was supported by EPSRC grant EP/R026173/1 for ORCA Hub project.

complexity, it may not be suitable for low-powered sensor nodes in UWASNs.

Owing to the fact that most natural phenomenon are compressible in an appropriate basis, e.g., smoothly varying field is sparse in frequency domain, the CS techniques have been exploited to mitigate the challenges point out earlier. The theory of CS states that under certain conditions, exact signal reconstruction is possible with only small number of random measurements [7], [8]. Thus, rather than gathering the sensed data sampled by all the sensor nodes at each time frame, only few random nodes need to transmit their measurements. This can reduce significantly the bandwidth and the energy consumption required for signal reconstruction. The first example application of CS in sensor networks was introduced in [9]. Since then, several works, including [10]–[14] have been published. While quite diverse in the issues addressed (e.g., routing, performance, compressive measurements), most of those works have considered terrestrial wireless sensor networks. As such, their results cannot be directly applied to UWASNs. Fatemeh et al. in [15] proposed random access compressed sensing (RACS) scheme for UWASNs, which is one of the most important work applying CS theory to mitigate the problems faced in data gathering and field reconstruction. Random access protocols in general are very simple to implement, as they do not require the scheduling of transmissions, as in TDMA protocols, nor do they need control signals to establish collision-free links, as in contention-based MAC protocols. More recently, [16], [17] proposed interleave-division multiple access (IDMA) based compressive sensing schemes. IDMA is an extension of CDMA inheriting the good features of CDMA, but also the power hungry high computational complexity, thus not suitable for long-term deployment in oceans.

For these reasons, in the proposed framework, we consider the random channel access scheme proposed in [15]. However, unlike the regular grid deployment of sensor nodes considered in that work, we consider random deployment of the sensor nodes over a given region ROI. Making no assumption on the location of the sensor nodes is key to support opportunistic deployments and generally increase the applicability of the monitoring framework. However, the sensor nodes must be localized before the sensing process can begin. Sensor network localization is a well studied topic; see [18], [19] for a surveys on network localization. Typically, a node localization is achieved in two steps: i) ranging from at least minimum number of reference nodes with known positions, referred to as *anchors*, and ii) then preforming trilateration or multilateration or relaxed convex optimization [20], [21].

For spatio-temporal field estimation from random measurements, we assume that the field is varying slowly with the time, i.e., the two consecutive frames are highly correlated to each other, which is often the case for natural phenomena we are interested in. An important key characteristic of our framework is that, unlike [15], we exploit this information in field estimation phase, and show by simulations that the number of sensors taking part in measurements and channel access during a frame reconstruction can be reduced drastically. Effectively, each sensor involves less frequently in sensing and transmitting measurements, thus prolonging the life-time of each sensor node.

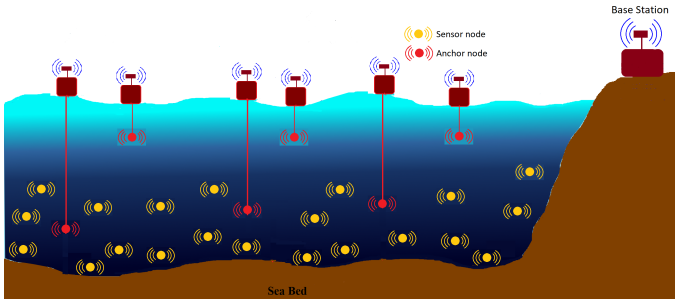

Fig. 1: A typical setting of proposed framework. Red are anchors and yellow are sensor nodes. Anchors nodes are surface buoys with acoustic modems handing from them at certain depth. The sensor nodes are randomly at different locations above the seabed. Fusion center lies on sea shore connected to anchors via radio channels.

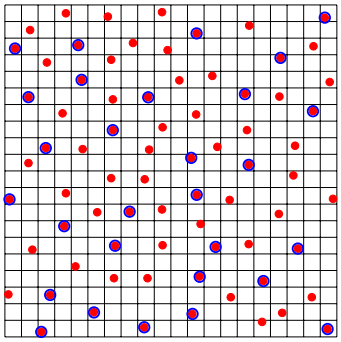

Fig. 2: Randomly deployed sensor nodes (in red) and the descretized space. Encircled in blue are randomly selected sensor nodes for measurement during a frame.

The remaining paper is organized as follow: In Section II we describe the framework with the network model. In Section III, we present the silent localization scheme with some simulation results showing its performance. In Section IV, we outline the spatio-temporal sensing based on compressive sensing and random channel access, and suggest suitable solution to the convex optimization algorithms for performing field reconstruction. We show by simulation result how temporal coherency can be exploited to prolong overall the life-time of the network. Finally, Section V draws our conclusions.

II. Underwater Monitoring Framework

Consider a UWASN of M static sensor nodes deployed uniformly at random over ROI. The proposed framework for remote monitoring of ocean environment is consists of three main phases: (i) deployment and localization of sensor nodes, (ii) random access of acoustic channel to transmit the sensor's measurements to the FC, and (iii) field reconstruction at the FC from correctly received measurements. The sensor network in our framework consists two types of nodes: few anchors and sufficiently many sensor nodes. The nodes have

their unique identifiers, independent (not synchronized) clocks and acoustic modem with omni-directional antenna. A typical scenario of our framework is shown in Fig.1. Anchors are deployed on the ocean surface with acoustic modems hanging few meters below the surface. Thus, anchors can have a sufficiently large power supply (probably supported by solar panels), a GPS module, a modem with long acoustic ranges and sufficiently powerful computing units. The anchors serve two purposes: as references for the sensors and gateways to the FC. The anchors can communicate with the FC at shore through radio channels, thus have very high bandwidths compared to underwater acoustic channel. One of the anchors is considered as a gateway. On other hand, the sensor nodes are deployed deep into the ocean, have relatively small acoustic ranges and less demanding computing units. Thus, they are suitable for powering up by small batteries that can last for long time (typically for several months).

The framework utilize two types of multiple access protocols: i) TDMA proposed in [6] for transmitting some critical information that should not be lost e.g., positions of sensors, and ii) random access proposed in [15] for transmitting measurements from sensors to the FC. After the localization phase, the sensors transmit their positions to the FC using TDMA. Knowing the positions of the sensors, the FC discretizes the space into N regular interval zones depending upon resolution required by the application. For example, see Fig. 2 where a 2-D space is discretized into regular interval zones where few of zones have at least a node. For sake of mathematical simplicity, we assumed that the nodes lie in the center of the zones.

In the proposed framework, we consider monitoring slowly (smoothly) varying fields both in the spatial and in the temporal domain. Similar to [15], we consider frame-based measurement transmission to the FC. Let T_{coh} be the coherence time of the monitored process over which the process almost decorrelates in time. Unlike [15], we chose a shorter frame duration $T < T_{\text{coh}}$ over which the process has sufficient correlation in time. The correlation between the consecutive frames is exploited to reduce the numbers of required measurements during reconstruction. The sensing process starts after the FC broadcasts the frame duration to the sensors. Every T frame duration, a subset of sensors is selected at random to conduct measurements; see Fig 2. This can be done by equipping the sensors with independent, identically distributed (i.i.d.) Bernoulli random generator. Each sensor determines whether it will participate in the sensing process with some probability. Total number of sensors selected for sampling in a frame is then a random variable with some Binomial distribution. The measurements are then transmitted to the FC using random access. Let T_{p} be the duration of data packet containing sensor measurement and the node identifier. Each node picks a random transmission delay uniformly in $[0, T - T_{\text{p}}]$ and transmits the packet to the gateway. In this random access, there is a possibility of collision of packets. A collision occurs if packets from different sensors overlap in time and interfere each other while reaching to the gateway. A key idea of the proposed framework is to let the gateways simply discard the colliding packets. Motivated by the theory of CS, the FC does not care what specific nodes were selected, as long as (i) the selected subset is chosen uniformly at random, and (ii) there are sufficiently many collision-free packets received to allow reconstruction of the frame. Let K denotes the numbers of collision-free packets received at the FC during one frame. This is a random variable who value depend upon the sensing probability of each sensor node. For small sensing probability, number of measurements will be small, thus less collisions, but poor quality of reconstruction. On the other hand, increasing sensing probability will result in large number of measurements that could improve the quality of reconstruction, but after certain limit, this will increase collisions of packets reaching the gateway. In order to minimize the overall energy consumption of the network, one has to select the smallest value of sensing probability while maintaining reasonable quality of reconstruction. Thus, there is trade-off in choosing sensing probability. For analytical study of probability distribution of K, please refer to [15].

III. Deployment and localization of sensor network

Traditional ways of capturing a spatio-temporal field, i.e., following the Nyquist sampling theory, would require deploying sensors at regular interval grids at least twice dense than the highest spatial frequency of the field. This can be very tedious and time consuming task [3], [4]. Theory of CS alleviates this: the framework consider the opportunistic random deployment of sensors. However, it necessitates to localize the sensors before starting sensing process. Localization needs minimum numbers of anchors with known positions. These anchors need to be deployed carefully in the ROI, such that they avoid certain geometric conditions and covers the ROI acoustically. We consider anchors lie on the sea surface with their acoustic modems are hanging in water. Few of them are hanging just few (1 to 2) meters deep, and few of them are hanging more deeper depending upon the depth of sensor nodes to be localized. Random deployment of large numbers of sensor nodes and few deliberate deployments of anchors is more economic than the traditional regular grid scheme. Moreover, if the nodes drifts over time, we can easily re-localize them, thanks to the positioning scheme we present below.

Sensor network localization techniques can be broadly classified into two categories: range-based and range-free. Range-based techniques measure or estimate distances to a small number of anchor nodes via time-of-arrival (ToA) or time-difference-of-arrival (TDoA) and then apply triangulation or multilateration or relaxed convex optimization [20], [21] to estimate the coordinates. The minimum necessary condition is that there should be at least three non-collinear anchors for 2-D space localization and at least four non-coplanar (and three of them should be non-collinear) for 3-D space localization. Range-free techniques explore the local topology and derive the position estimate from the location of surrounding anchor nodes. Generally, range-based techniques provide better position accuracy than range-free localization.

ToA or TDoA approaches require time synchronization if one-way sound flying time is counted on; otherwise, a ping-pong-style round trip propagation delay needs to be measured. In underwater environment, precise time synchronization among the nodes is hard to achieve due to the characteristics of sound wave in water [3]. Due to long propagation delay of acoustic signal, the ping-pong-style needs long time before all sensor nodes finish pinging all the anchors. In this paper, we present UPS, a silent positioning scheme first proposed in [22], and suggest geometrical configurations of the anchors to cover large localizable space and easy extension of the localizable space.

A. Silent positioning scheme

Here, we present the details of the UPS for UWASNs in 3D space. UPS requires very few anchors (three for 2-D space and four for 3-D space) with long-range beacons signal. Three anchors lie on the surface and one lies deep into ocean. Example of geometric configuration of anchors are shown in first row of the Fig. 7. The anchors and the sensors have their own local timers and do not need synchronization among them. UPS consists of two steps: (i) sensor nodes detect TDoAs from the four anchors and transform them into range differences, and (ii) sensors do trilateration to transform these range estimates into coordinates.

Consider the four anchors A, B, C, D, and a sensor S to be localized. Let $\boldsymbol{x}_i = \left[x_i, y_i, z_i\right]^{\mathrm{T}},\ i \in \{\mathrm{A}, \mathrm{B}, \mathrm{C}, \mathrm{D}\}$ be the coordinates of the anchors. Let $\boldsymbol{x} = [x, y, z]^{\mathrm{T}}$ the coordinate of the S. Let d_i be distance between sensor S and each anchor nodes $i \in \{\mathrm{A}, \mathrm{B}, \mathrm{C}, \mathrm{D}\}$.

First step of UPS computes the range differences between d_{A} and $d_{\mathrm{B}}, d_{\mathrm{C}}, d_{\mathrm{D}}$, respectively.

Step 1—Range Difference Computation: Let A be the master anchor, which initiates a beacon signal. At times $t_1, t_{\mathrm{B}}, t_{\mathrm{C}}$, and t_{D} the sensor S and anchors B, C, and D receive the beacon signal, respectively. At time $\tilde{t}_{\mathrm{B}} \geq t_{\mathrm{B}}$ B replies anchor A with a beacon signal conveying information $\tilde{t}_{\mathrm{B}} - t_{\mathrm{B}} = \Delta t_{\mathrm{B}}$. This signal reaches S at time t_2. After receiving signal from A and B, at time $\tilde{t}_{\mathrm{C}}$, C replies to A with a beacon signal conveying information $\tilde{t}_{\mathrm{C}} - t_{\mathrm{C}} = \Delta t_{\mathrm{C}}$. This signal reaches S at t_3. After receiving signal from A, B, and C, at time $\tilde{t}_{\mathrm{D}}$ D replies to A with a beacon signal conveying information $\tilde{t}_{\mathrm{D}} - t_{\mathrm{D}} = \Delta t_{\mathrm{D}}$. This signal reaches S at time t_4. Based on triangle inequality, $t_1 < t_2 < t_3 < t_4$. Note that all the arrival times are measured locally. Let the TDoA be $\Delta t_1 = t_2 - t_1,\ \Delta t_2 = t_2 - t_1,\ \Delta t_3 = t_3 - t_1$. Then, the range differences will be

$$\begin{aligned}
\Delta d_{\mathrm{B}} &= d_{\mathrm{A}} - d_{\mathrm{B}} = d_{\mathrm{AB}} + v \cdot (\Delta t_{\mathrm{B}} - \Delta t_1) \\
\Delta d_{\mathrm{C}} &= d_{\mathrm{A}} - d_{\mathrm{C}} = d_{\mathrm{AC}} + v \cdot (\Delta t_{\mathrm{C}} - \Delta t_2) \\
\Delta d_{\mathrm{D}} &= d_{\mathrm{A}} - d_{\mathrm{D}} = d_{\mathrm{AD}} + v \cdot (\Delta t_{\mathrm{D}} - \Delta t_3)
\end{aligned}$$

where v is velocity of sound, and $d_{\mathrm{AB}}, d_{\mathrm{AC}}, d_{\mathrm{AD}}$ are ranges between anchor A and the remaining anchors B, C, and D, respectively.

The second step involves computing coordinates using the range differences. This step is computationally inexpensive: just involves inverting a 3×3 matrix and finding a square-root. Thus, it can implemented on low-powered processing unit.

Step 2—Location Computation: We have:

$$d_{\mathrm{A}}^2 = (\boldsymbol{x} - \boldsymbol{x}_{\mathrm{A}})^2 \Rightarrow\ \boldsymbol{x}^2 - d_{\mathrm{A}}^2 - 2\boldsymbol{x}_{\mathrm{A}}^{\mathrm{T}}\boldsymbol{x} + \boldsymbol{x}_{\mathrm{A}}^2 = 0 \quad (1)$$

where we represent $\boldsymbol{x}^{\mathrm{T}}\boldsymbol{x} = \boldsymbol{x}^2$.
And for $i \in \mathrm{B}, \mathrm{C}, \mathrm{D}$

$$\begin{aligned}
&(d_{\mathrm{A}} - \Delta d_i)^2 = d_i^2 = (\boldsymbol{x} - \boldsymbol{x}_i)^2 \\
&\Rightarrow \boldsymbol{x}^2 - d_{\mathrm{A}}^2 - 2\boldsymbol{x}_i^{\mathrm{T}}\boldsymbol{x} + 2\Delta d_i d_{\mathrm{A}} + \boldsymbol{x}_i^2 - \Delta d_i^2 = 0 \quad (2)
\end{aligned}$$

By subtracting (1) from (2), we obtain, for $i \in \{\mathrm{B}, \mathrm{C}, \mathrm{D}\}$:

$$2(\boldsymbol{x}_{\mathrm{A}} - \boldsymbol{x}_i)^{\mathrm{T}}\boldsymbol{x} + 2\Delta d_i d_{\mathrm{A}} + \boldsymbol{x}_i^2 - \Delta d_i^2 - \boldsymbol{x}_{\mathrm{A}}^2 = 0 \quad (3)$$

This system of linear equations can be expressed as:

$$\mathbf{M} \cdot \boldsymbol{x} + d_{\mathrm{A}}\boldsymbol{c} + \boldsymbol{d} = \mathbf{0} \quad (4)$$

where

$$\begin{aligned}
\mathbf{M} &= \begin{bmatrix} 2(x_{\mathrm{A}} - x_{\mathrm{B}}) & 2(y_{\mathrm{A}} - y_{\mathrm{B}}) & 2(z_{\mathrm{A}} - z_{\mathrm{B}}) \\ 2(x_{\mathrm{A}} - x_{\mathrm{C}}) & 2(y_{\mathrm{A}} - y_{\mathrm{C}}) & 2(z_{\mathrm{A}} - z_{\mathrm{C}}) \\ 2(x_{\mathrm{A}} - x_{\mathrm{D}}) & 2(y_{\mathrm{A}} - y_{\mathrm{D}}) & 2(z_{\mathrm{A}} - z_{\mathrm{D}}) \end{bmatrix}, \\
\mathbf{c} &= \begin{bmatrix} 2\Delta d_B \\ 2\Delta d_C \\ 2\Delta d_D \end{bmatrix}, \\
\mathbf{d} &= \begin{bmatrix} x_{\mathrm{B}}^2 + y_{\mathrm{B}}^2 + z_{\mathrm{B}}^2 - \Delta d_{\mathrm{B}}^2 - x_{\mathrm{A}}^2 - y_{\mathrm{A}}^2 - z_{\mathrm{A}}^2 \\ x_{\mathrm{C}}^2 + y_{\mathrm{C}}^2 + z_{\mathrm{C}}^2 - \Delta d_{\mathrm{C}}^2 - x_{\mathrm{A}}^2 - y_{\mathrm{A}}^2 - z_{\mathrm{A}}^2 \\ x_{\mathrm{D}}^2 + y_{\mathrm{D}}^2 + z_{\mathrm{D}}^2 - \Delta d_{\mathrm{D}}^2 - x_{\mathrm{A}}^2 - y_{\mathrm{A}}^2 - z_{\mathrm{A}}^2 \end{bmatrix}
\end{aligned}$$

Let $\boldsymbol{a}, \boldsymbol{b}$ be vectors such that:

$$\mathbf{M} \cdot \boldsymbol{a} + \boldsymbol{c} = 0 \text{ and } \mathbf{M} \cdot \boldsymbol{b} + \boldsymbol{d} = 0 \quad (5)$$

Let $\tilde{\boldsymbol{x}} = \boldsymbol{x} - \boldsymbol{b}$, then using (4) we get :

$$\begin{aligned}
&\mathbf{M}(\tilde{\boldsymbol{x}} + \boldsymbol{b}) + d_{\mathrm{A}}\boldsymbol{c} + \boldsymbol{d} = 0 \\
&\text{using (5) we get } \mathbf{M}\tilde{\boldsymbol{x}} + d_{\mathrm{A}}\boldsymbol{c} = 0\ \Rightarrow \tilde{\boldsymbol{x}} = d_{\mathrm{A}}\boldsymbol{a}
\end{aligned}$$

Thus, we have:

$$\boldsymbol{x} = d_{\mathrm{A}}\boldsymbol{a} + \boldsymbol{b} \quad (6)$$

From (1) and (6), we get:

$$(\boldsymbol{a}^2 - 1)d_A^2 + 2\boldsymbol{a}^{\mathrm{T}}(\boldsymbol{b} - \boldsymbol{x}_{\mathrm{A}})d_{\mathrm{A}} + (\boldsymbol{b}^2 + \boldsymbol{x}_{\mathrm{A}}^2) = 0 \quad (7)$$

Coordinate of S is found by these steps:

1) Solve (5) to obtain the vectors $\boldsymbol{a}$ and $\boldsymbol{b}$
2) Solve the quadratic equation (7) to obtain the range d_{A}
3) If one positive solution exits, then use (6) to obtain the coordinate $\boldsymbol{x}$ of S, otherwise no unique solution exists.

If (7) does have two positive solutions, we can use some sanity check to eliminate one of the solution, e.g., if the sensor node has depth sensor, then we can eliminate the infeasible solution.

The errors in measurements of TDoA are inevitable, and can occur due to the noise in the electronics, Doppler effect, variable acoustic speed underwater and multipath. In order to minimize the effects of the errors in TDoA, we can repeat the beacon signaling cycle described in *Step 1* and have several copies of the range differences $\Delta d_{\mathrm{i}}, i = \{B, C, D\}$, and use their average (assuming errors from i.i.d. Gaussian distributions) or median (assuming errors are from i.i.d. uniform distributions). The latter is often the case since the errors due

to variable acoustic speed and multipath can be approximately modeled by Uniform distribution. Please refer to [22], [23] for further discussion on sources of errors and theoretical error analysis. Note how in the case that the sensor nodes drift slowly over the time, the beacon signaling cycle can be easily repeated to re-estimate their location. At the end of the localization phase, the estimated locations of the nodes are transmitted to the FC using TDMA [6].

	Numbers of localized nodes			
Depth	Config #1	Config #2	Config #3	Config #4
15	318	269	292	311
50	339	257	313	317
150	377	239	354	340
350	373	262	400	375
500	377	253	398	391
800	398	214	400	400
1200	400	152	400	400

TABLE I: Number of nodes localized out of 400 nodes on regular grid over region $[-2000, 2000] \times [-2000, 2000]$ in planes at different depth in meters.

	iid Gaussian noise with STD σ		iid Uniform noise within $[-\sqrt{3}\sigma, \sqrt{3}\sigma]$	
σ	RMSE	#localized nodes	RMSE	#localized nodes
0.0012	33.2259	3887.4	39.3305	3880.7
0.0025	57.2272	3866	71.1845	3850.2
0.005	99.4818	3828.5	124.4996	3802.5
0.0075	142.7852	3794.9	181.3364	3769.5

TABLE II: Effect on of noise in TDoA measurments: Average RMSE in estimated locations (performed over 10 simulations) and Number of nodes localized out of total 4000 nodes spread in the space defined by $[-2000, 2000] \times [-2000, 2000] \times [50, 2000]$. Distances are in meters.

B. Simulation: Localization

The location estimated using TDoA is given by intersection of 3-D hyperboloids whose foci are the anchors. Uniquely localizable space around the anchors depends upon the geometric configuration of the anchors. The anchors should be placed such that it covers maximum space where the sensors can be localized uniquely while being in acoustic ranges of the anchors. Finding an optimal configuration of anchors for a given ROI and acoustic ranges of the anchors is a difficult problem. Thus, we conducted simulation to find uniquely localizable space for different practically deployable geometric configurations. In our simulation, we considered three anchors A, B, C on the surface and the fourth anchor D at certain depth below surface. All the anchors have acoustic range of 4000 meters. No noise was introduced in the TDoA measurements. In Fig. 7, we show only the four configurations, namely Config #1, Config #2, Config #3, and Config #4 and their uniquely localizable spaces. We considered 400 sensors at regular grid within 2-D region defined by $[-2000, 2000] \times [-2000, 2000]$ lying at different depths. In the first three configurations, the surface anchors form equilateral triangle with a side length of 1000 meters, while in the last configuration, they form right-angled triangle with two sides of length 1000 meters. In all configurations, the fourth anchor lies at depth of 500 meters. We can see that the space very near to any anchor is not localizable, but after certain depth, the Config #1 and Config #3 cover largest symmetrical localizable space, while Config #4 covers unsymmetrical localizable space, which may not be suitable in the case when anchors have omnidirectional acoustic range. The Config #2 has the smallest localizable space. Table I shows the number of localized nodes out of 400 nodes at different depths. We found that the optimal configurations is the one when the surface anchors form an equilateral triangle and the fourth anchor has certain offset from their centroid. Any variation from this configuration resulted in shrinking the localizable space. Moreover, it is important to note that the sensor nodes lying below the depth of the anchor D are localizable, thus it is not necessary to deploy the anchor D very deep in order to localize deeper sensor nodes.

We also studied the effect of errors in TDoA measurements. We considered two types of statistical source of errors: i.i.d. Gaussian and i.i.d. Uniform distribution. In the simulation, we considered $N = 4000$ sensor nodes spread over a regular grid within the space defined by $[-2000, 2000] \times [-2000, 2000] \times [50, 2000]$, and Config #1 for the anchors. Speed of the sound in water was considered to be 1500 meters/sec, i.e. an error of 1 millisecond corresponds to 1.5 meters. The locations of the nodes were estimated using measurements taken over five beacon signaling cycles. The Table II presents the results of simulation: root-mean-square-error $\left(RMSE = \sqrt{\frac{\sum_{i=1}^{N} \|\boldsymbol{x}_i - \hat{\boldsymbol{x}}_i\|_2^2}{N}} \right)$ in the estimated locations and the number localized nodes out 4000 nodes. We see that repeating the beacon signaling for certain number of cycles mitigates very well the effect of errors in measurements. Moreover, we can easily increase our confidence on the estimated locations by comparing the results from few different configurations, e.g. Config #1 and Config #2, at expense of adding few more anchors as D. This will also extend the localizable space. In fact, extending the localizable space to an existing network can be easily accomplished by adding few more anchors to a existing configuration. e.g. by deploying a surface and an underwater anchor node, and including the new anchors into the beacon signaling cycles.

IV. Spatio-temporal Sensing

In Section II we described a generic scenario and sensor node localization in 3-D space, but here, we consider 2-D space for demonstrating the spatio-temporal sensing, which can be easily extended to 3-D space. For this, let assume that the ROI is discretized in to $I \times J = N$ regular interval zones over which M sensor nodes are deployed uniformly at random. During a frame, let K collision free measurements $\boldsymbol{y} \in \mathbb{R}^K$ reach to the FC. Let $\boldsymbol{u} \in \mathbb{R}^N$ denotes the field map we like to estimate from the measurements. Note we denote a 2-D field (matrix) as a vector by stacking its columns.

The measurements from uniformly at random sensors can be modeled as:

$$\boldsymbol{y} = \boldsymbol{\Phi u} \tag{8}$$

where $\boldsymbol{\Phi} \in \mathbb{R}^{K\times N}$ is sensing matrix consist of K rows of an identity matrix selected uniformly at random. This random sensing matrix accounts for both the randomly selected sensors for measurement and random collisions at FC. If the field $\boldsymbol{u}$ is sparse in a representation basis $\boldsymbol{\Psi} \in \mathbb{R}^{N\times N}$, then we have $\boldsymbol{u} = \boldsymbol{\Psi v}$, where $\boldsymbol{v}$ has very few non-zero elements. The theory of CS [7], [8] states that as long as the field is S-sparse in the representation basis $\boldsymbol{\Psi}$ and K correctly received measurements, picked uniformly at random, is greater than $N_s = CS\log N$, then with very high probability the field $\boldsymbol{u}$ can be estimated exactly by solving the following convex optimization:

$$\arg\min_{\hat{\boldsymbol{v}}} \|\hat{\boldsymbol{v}}\|_1 \;\text{ subject to } \boldsymbol{y} = \boldsymbol{\Phi\Psi}\hat{\boldsymbol{v}} \tag{9}$$

$$\hat{\boldsymbol{u}} = \boldsymbol{\Psi}\hat{\boldsymbol{v}} \tag{10}$$

Here C is a constant independent of both N and S. Moreover, we also assume that the matrix $\boldsymbol{\Phi\Psi}$ admits the *restricted isometry property* (RIP) [7]. With high probability, a random sensing matrix such as $\boldsymbol{\Phi}$ in our case achieves RIP. The optimization problem (9) is referred to as *basis pursuit* [24] and can be solved efficiently by plenty of solvers, e.g. see [25], [26, p. 41] and references within.

Usually, the fields are not exactly sparse but nearly sparse. Moreover, the measurements contains some noise due to characteristics of sensors. Under this condition the observation model is written as:

$$\boldsymbol{y} = \boldsymbol{\Phi u} + \boldsymbol{e} \tag{11}$$

where we consider $\boldsymbol{e}$ to be i.i.d. Gaussian noise. CS theory still guarantees that the field can be recovered with good accuracy by solving the following convex optimization:

$$\arg\min_{\hat{\boldsymbol{v}}} \|\hat{\boldsymbol{v}}\|_1 \;\text{ subject to } \|\boldsymbol{y} - \boldsymbol{\Phi\Psi}\hat{\boldsymbol{v}}\|_2 \le \epsilon \tag{12}$$

where $\epsilon > 0$ bounds the amount of the noise in the measurements. This is usually referred to as *robust signal recovery* problem. Problem (12) can also be equivalently written as:

$$\arg\min_{\hat{\boldsymbol{v}}} \frac{1}{2}\|\boldsymbol{y} - \boldsymbol{\Phi\Psi}\hat{\boldsymbol{v}}\|_2^2 + \lambda\|\hat{\boldsymbol{v}}\|_1 \tag{13}$$

where $\lambda > 0$ is a regularization parameter to balance the twin objectives of minimizing the error and sparsity, and is directly proportional to the strength of noise in the measurements. This *regularized reconstruction* (13) is usually preferable over the previous formulation (12) for it can be efficiently solved by solvers in [26]–[30] given that representation basis $\boldsymbol{\Psi}$ admits a fast matrix-vector multiplication.

In this paper, we choose Discrete Cosine Transform (DCT) as representation basis $\boldsymbol{\Psi}$ for it can sparsely represent the smoothly varying field and admits a fast matrix-vector multiplication using Fast Fourier Transform [31]. As discussed above, along with exploiting the smoothness of the field in spatial domain, we also exploit the smoothness of the slowly varying field along temporal domain. Two consequent frames of a slowly varying field have high correlation between them with overwhelming probability. Thus, given that we have the estimate of the previous $(t-1)$-th frame, we propose to reconstruct t-th frame by solving following optimization:

$$\arg\min_{\hat{\boldsymbol{v}}_t} \frac{1}{2}\|\boldsymbol{y}_t - \boldsymbol{\Phi}_t\boldsymbol{\Psi}\hat{\boldsymbol{v}}_t\|_2^2 + \lambda\|\hat{\boldsymbol{v}}_t\|_1 + \frac{\zeta}{2}\|\hat{\boldsymbol{v}}_t - \hat{\boldsymbol{v}}_{t-1}\|_2^2 \tag{14}$$

get the estimated frame as $\hat{\boldsymbol{u}}_t = \boldsymbol{\Psi}\hat{\boldsymbol{v}}_t$. In this above formulation, the closeness between two consequent frames is imposed by the third term and parameter $\zeta \ge 0$ controls its effect; higher value of ζ imposes higher correlation between two consequent frames.

A. Simulation: Field Reconstruction

To validate the proposed spatio-temporal field reconstruction, we considered synthetic temperature field consists of 500 frames of spatial dimension of $42\times 42 = 1764$ zones. The field varies smoothly along the spatial and temporal domain except at every hundredth frame there are bumps of temperature spots at random locations; see Fig. 8, which shows the different frames. We considered 1323 sensor nodes deployed uniformly at random in those zones. During each frame a subset sensor nodes selected uniformly at random perform measurements and transmit them to the FC. We define *compression ratio* c as number of correctly received measurements at FC during a frame divided by total number of zones in the field. To measure the quality of reconstructed field, we used root-mean-square-error (RMSE) criterion defined as $\sqrt{\frac{\|\boldsymbol{u}_t - \hat{\boldsymbol{u}}_t\|_2^2}{N}}$. To solve the optimization problem (9), we used the ADMM presented in [26, Sec 6.2] and for problems (13) and (14), we used FISTA with backtracking proposed in [28, Sec 3].

For a given field, the minimum number of measurements N_s required to reconstruct the field with high accuracy is a prerequisite to perform compressive sensing. Since in our simulation, the field is changing with time, N_s cannot be the same for all the frames. Thus, the first task is to find a value of N_s that will result good quality reconstruction over all the frames. To do so, we selected few random frames and reconstructed them individually by solving the problem (12) for different values of compression ratio c during the measurements. We found $c = 0.25$ i.e., $N_s = 441$ is well suited for all the frames as shown in the plot in Fig. 3. Increasing further the value of c did not significantly changed RMSE of the reconstructed frames.

Next, we considered reconstruction from noisy measurements. The temperature field in our simulation varies between 5 to 20 degree Celsius. During the sensing phase, we fixed $c = 0.25$ and corrupted the measurements in each frame by i.i.d. Gaussian noise with zero mean and standard deviation ($\sigma = 0.25$). In this case, the frames are reconstructed by solving problem (14). We did *warm-starts* of the FISTA algorithm for the reconstruction of the consecutive frames. Here, we have two parameters λ and ζ to be tuned to achieve good quality of reconstruction. To find best values the two parameters, we performed a grid-search in (λ, ζ) space: we fixed the value of ζ and reconstructed the frames for different

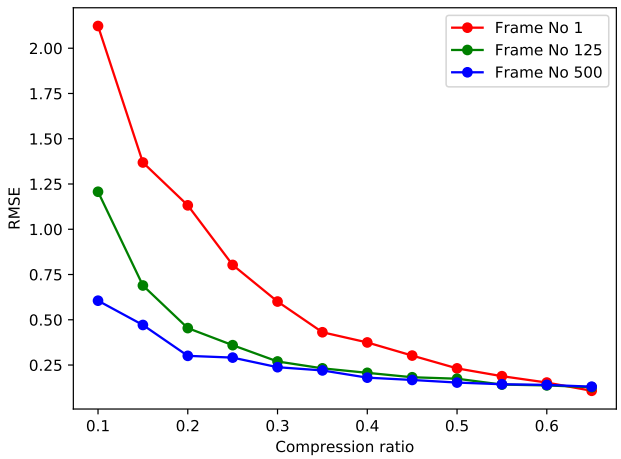

Fig. 3: Selecting sufficient compression ratio c to obtain adequate reconstruction quality over all the frames. $c = 0.25$ produces reasonable quality for most of the frames.

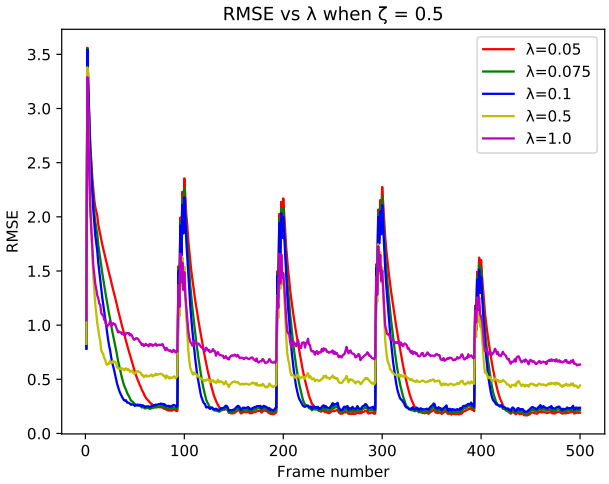

Fig. 4: Selecting regularization parameter λ for best reconstruction from noisy measurements. $\lambda = 0.1$ is possibly the optimal value.

values of λ, and repeated this for different values of ζ. We found that the pair $\lambda = 0.1, \zeta = 0.5$ resulted the best possible reconstruction i.e. the lowest RMSE over all frames. Figure 4 shows the RMSE for all the frames for different values of λ when ζ is fixed at 0.5. Similarly, Fig. 5 shows the RMSE for all the frames for different values of ζ when λ is fixed at 0.1. From the latter plots, we can easily see that the quality of reconstruction drastically improves when we impose the correlation betweens the consecutive frames. This indicates that including the information from previous frame into the reconstruction of current can lower the number of measurements required to reconstruct the consecutive frames. This is confirmed by the plots in Fig. 6, which shows that we need to increase the value of c to 0.6 when using no information from previous frame, i.e., $\zeta = 0$, to achieve the similar quality of reconstruction when $c = 0.25$ and $\zeta = 0.5$. This validates experimentally our proposed compressive sensing scheme, which requires less number of measurements and collisions, and thus prolongs the life-time of each sensor node. We also see bumps in RMSE in the plots at the certain frames (e.g., at frame number 100, 200, 300, and 400). This is due to the fact that the temperature field changes drastically at those frames. In Figure 5, we see that for smaller values of ζ, the reconstruction recovers quickly from those bumps effects, but the RMSE remains higher for all the frames, whereas for the larger values of ζ, the reconstruction recovers slowly, but reaches to lower value of RMSE. There is always a trade-off, and one can select the value of ζ depending upon the application, but it is always preferable to choose $\zeta > 0$.

V. Conclusion

We presented a framework for spatio-temporal monitoring of ocean environment by UWASNs. The spatio-temporal field reconstruction is based on compressive sensing, which allows random deployment of the sensor nodes in the ROI, perform random measurements and use random channel access to

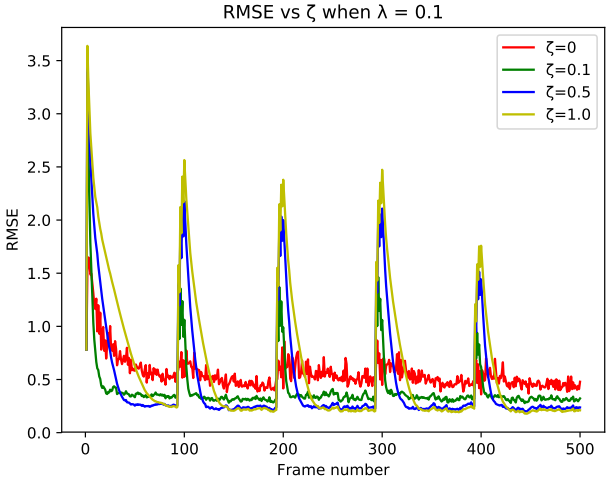

Fig. 5: Selecting regularization parameter ζ for best reconstruction from noisy measurements. $\zeta = 0.5$ is possibly the optimal value.

transmit the data to a FC. To this end,we considered a silent positioning scheme for randomly deployed sensors, and studied optimal geometric configurations of anchor nodes to maximise the localizable space. For slowly varying field, there is high correlation between consecutive frames. We proposed to utilize this information during reconstruction of consecutive frames. This resulted in a significant reduction of the required number of measurements needed to achieve reasonable quality of the estimated field. Utilizing silent positioning for sensor nodes and compressive sensing for spatio-temporal field reconstruction from randomly collected measurements save both energy and bandwidth, which ultimately enables long-term deployment of UWASNs.

In sensing phase, we chose the value of the regularization parameter ζ empirically. Future work will try to theoretically

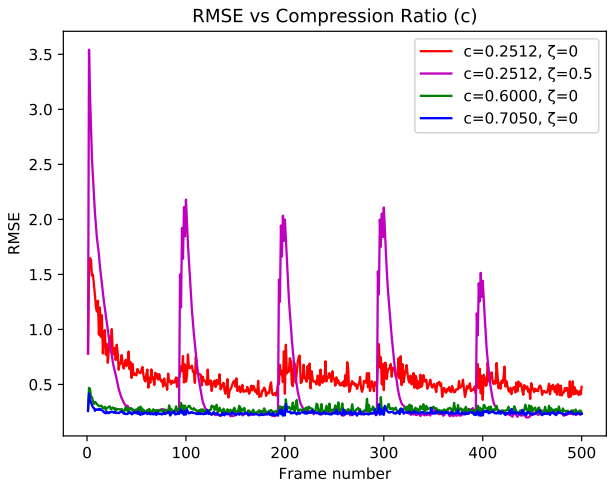

Fig. 6: Effect of including information from last frame into reconstruction of current frame. When $\zeta = 0$, we need to decrease compression 0.6 to achieve same quality of reconstruction when $\zeta = 0.5$ and $c = 0.25$.

predict its value based on correlation between previously reconstructed frames. Rather than using a centralized gathering of measurements and field reconstruction, we think that a distributed field reconstruction algorithm can mitigate the problems with centralized processing scheme. For example, each anchor may act as a local fusion center and collaborate with each other for global field reconstruction. Based on the simulation results, we are presently developing the hardware and the software needed for real-time deployment of the proposed framework.

REFERENCES

[1] E. M. Sozer, M. Stojanovic, and J. G. Proakis, "Underwater acoustic networks," *IEEE Journal of Oceanic Engineering*, vol. 25, no. 1, pp. 72–83, Jan 2000.

[2] L. Lui, S. Zhou, and J.-H. Cui, "Prospect and problems of wireless communication for underwater sensor networks," *Wireless Communications and Mobile Computing*, vol. 8, no. 8, pp. 977–994, 2008.

[3] J. Heidemann, M. Stojanovic, and M. Zorzi, "Underwater sensor networks: Applications, advances and challenges," *Philosophical Transactions of the Royal Society A: Mathematical, Physical and Engineering Sciences*, vol. 370, no. 1958, pp. 158–175, 2012.

[4] I. F. Akyildiz, D. Pompili, and T. Melodia, "Challenges for efficient communication in underwater acoustic sensor networks," *ACM SIGBED Review*, vol. 1, no. 2, pp. 3–8, 2004.

[5] D. Pompili and I. F. Akyildiz, "Overview of Networking Protocols for Underwater Wireless Communications," *IEEE Communications Magazine*, vol. 47, no. 1, pp. 97–102, 2009.

[6] N. Morozs, P. Mitchell, and Y. Zakharov, "TDA-MAC: TDMA Without Clock Synchronization in Underwater Acoustic Networks," *IEEE ACCESS*, vol. 6, pp. 1091–1108, 2018.

[7] E. J. Candès, J. K. Romberg, and T. Tao, "Stable signal recovery from incomplete and inaccurate measurements," *Communications on Pure and Applied Mathematics*, vol. 59, no. 8, pp. 1207–1223, 2006.

[8] E. Candes and M. Wakin, "An Introduction To Compressive Sampling," *IEEE Signal Processing Magazine*, vol. 25, no. 2, pp. 21–30, 2008.

[9] W. Bajwa, J. Haupt, A. Sayeed, and R. Nowak, "Compressive wireless sensing," in *International Conference on Information Processing in Sensor Networks*. Nashville, TN, USA: IEEE, 2006.

[10] C. T. Chou, R. Rana, and W. Hu, "Energy efficient information collection in wireless sensor networks using adaptive compressive sensing," in *Conference on Local Computer Networks*, Oct 2009, pp. 443–450.

[11] W. Chen and I. J. Wassell, "Energy efficient signal acquisition via compressive sensing in wireless sensor networks," in *International Symposium on Wireless and Pervasive Computing*, Feb 2011, pp. 1–6.

[12] C. Karakus, A. C. Gurbuz, and B. Tavli, "Analysis of energy efficiency of compressive sensing in wireless sensor networks," *IEEE Sensors Journal*, vol. 13, no. 5, pp. 1999–2008, May 2013.

[13] T. Xue, X. Dong, and Y. Shi, "Multiple access and data reconstruction in wireless sensor networks based on compressed sensing," *IEEE Transactions on Wireless Communications*, vol. 12, no. 7, pp. 3399–3411, July 2013.

[14] M. A. Razzaque and S. Dobson, "Energy-efficient sensing in wireless sensor networks using compressed sensing," *Sensors (Switzerland)*, vol. 14, no. 2, pp. 2822–2859, 2014.

[15] F. Fazel, M. Fazel, and M. Stojanovic, "Random access compressed sensing for energy-efficient underwater sensor networks," *IEEE Journal on Selected Areas in Communications*, vol. 29, no. 8, pp. 1660–1670, 2011.

[16] G. Liu and W. Kang, "IDMA-based compressed sensing for ocean monitoring information acquisition with sensor networks," *Mathematical Problems in Engineering*, vol. 2014, no. 1, 2014.

[17] W. Kang, R. Du, and G. Liu, "Dual-domain compressed sensing method for oceanic environmental elements collection with underwater sensor networks," *Mobile Networks and Applications*, vol. 23, no. 2, pp. 272–284, Apr 2018. [Online]. Available: https://doi.org/10.1007/s11036-017-0947-1

[18] G. Mao, B. Fidan, and B. D. Anderson, "Wireless sensor network localization techniques," *Computer Networks*, vol. 51, no. 10, pp. 2529 – 2553, 2007.

[19] Q. U. Fengzhong, W. Shiyuan, W. U. Zhihui, and L. I. U. Zubin, "A survey of ranging algorithms and localization schemes in underwater acoustic sensor network," *China Communications*, vol. 13, no. 3, pp. 66–81, 2016.

[20] L. Doherty, K. S. J. pister, and L. E. Ghaoui, "Convex position estimation in wireless sensor networks," in *Proceedings IEEE INFOCOM 2001. Conference on Computer Communications*, vol. 3, April 2001, pp. 1655–1663 vol.3.

[21] C. Soares, J. Xavier, and J. Gomes, "Simple and fast convex relaxation method for cooperative localization in sensor networks using range measurements," *IEEE Transactions on Signal Processing*, vol. 63, no. 17, pp. 4532–4543, Sept 2015.

[22] X. Cheng, A. Thaeler, G. Xue, and D. Chen, "Tps: a time-based positioning scheme for outdoor wireless sensor networks," in *IEEE INFOCOM 2004*, vol. 4, March 2004, pp. 2685–2696 vol.4.

[23] X. Cheng, H. Shu, Q. Liang, and D. H.-C. Du, "Silent positioning in underwater acoustic sensor networks," *IEEE Transactions on Vehicular Technology*, vol. 57, no. 3, pp. 1756–1766, 2008.

[24] S. S. Chen, D. L. Donoho, and M. A. Saunders, "Atomic Decomposition by Basis Pursuit," *SIAM Review*, vol. 43, no. 1, pp. 129–159, 2001.

[25] J. A. Tropp and S. J. Wright, "Computational Methods for Sparse Solution of Linear Inverse Problems," *Proceedings of IEEE*, vol. 98, no. 6, pp. 948–958, 2010.

[26] S. Boyd, N. Parikh, E. Chu, B. Peleato, and J. Eckstein, "Distributed Optimization and Statistical Learning via the Alternating Direction Method of Multipliers," *Foundation and Trends in Machine Learning*, vol. 3, no. 1, pp. 1–122, 2010.

[27] E. J. Candès and J. K. Romberg, "l1-magic: Recovery of Sparse Signals via Convex Programming," California Institute of Technology, Pasadena, CA, Tech. Rep., 2005. [Online]. Available: https://statweb.stanford.edu/ candes/l1magic/

[28] A. Beck and M. Teboulle, "A Fast Iterative Shrinkage-Thresholding Algorithm," *Society for Industrial and Applied Mathematics Journal on Imaging Sciences*, vol. 2, no. 1, pp. 183–202, 2009.

[29] S. J. Wright, R. D. Nowak, and M. A. Figueiredo, "Sparse reconstruction by separable approximation," *IEEE Transactions on Signal Processing*, vol. 57, no. 7, pp. 2479–2493, 2009.

[30] R. Mourya, L. Denis, J. Becker, and E. Thibaut, "Augmented lagrangian without alternating directions: Practical algorithms for inverse problems in imaging," in *International Conference on Image Processing*, Sept 2015, pp. 1205–1209.

[31] S. G. Johnson and M. Frigo, "A modified split-radix FFT with fewer arithmetic operations," *IEEE Trans. Signal Processing*, vol. 55, no. 1, pp. 111–119, 2007.

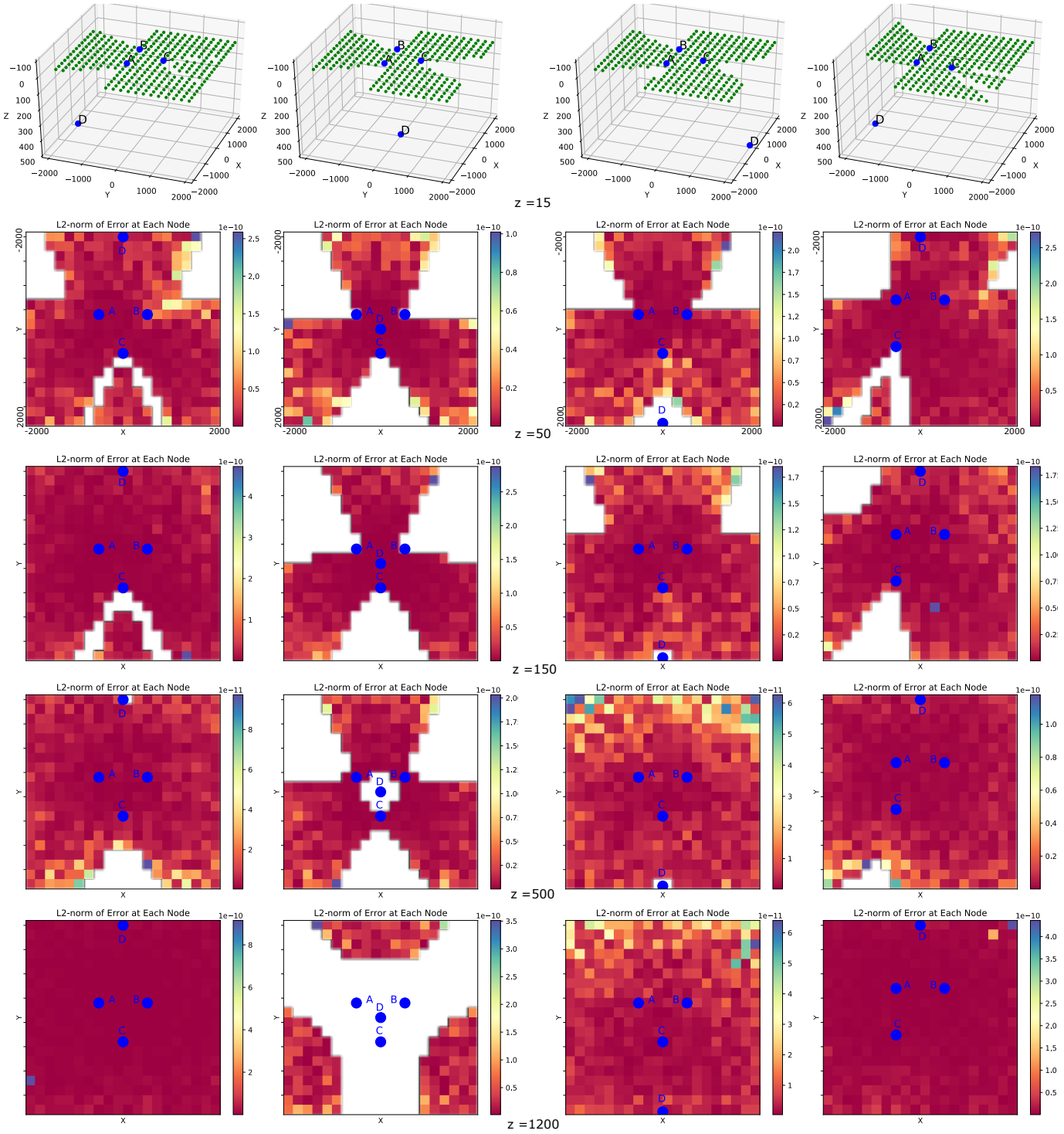

Fig. 7: Uniquely localizable space for four configurations of anchors: From left to right column: Config #1, Config #2, Config #3 and Config #4. Top row shows 3-D positions of anchors and localized sensors lying in plane $z = 15$. In the first three configurations, anchor A, B, C are located on the surface at $[-500, -288, 0], [500, -288, 0], [0, 578, 0]$, respectively, forming equilateral triangle, and D is located underwater at $[0, -2000, 500]$, $[0, 0, 500]$, and $[0, 2000, 500]$, respectively. In Config #4, A, B, C are at $[-500, -500, 0], [500, -500, 0], [-500, 500, 0]$, respectively forming right-angled triangle, and D is located at $[0, -2000, 500]$. 400 sensors are spread over the region $[-2000, 2000] \times [-2000, 2000]$. All the distances are expressed in meters. The maps in second row to till last row show the uniquely localizable space in different planes at depths $z = \{50, 150, 500, 1200\}$. No errors/noise were introduced in the TDoA measurements.

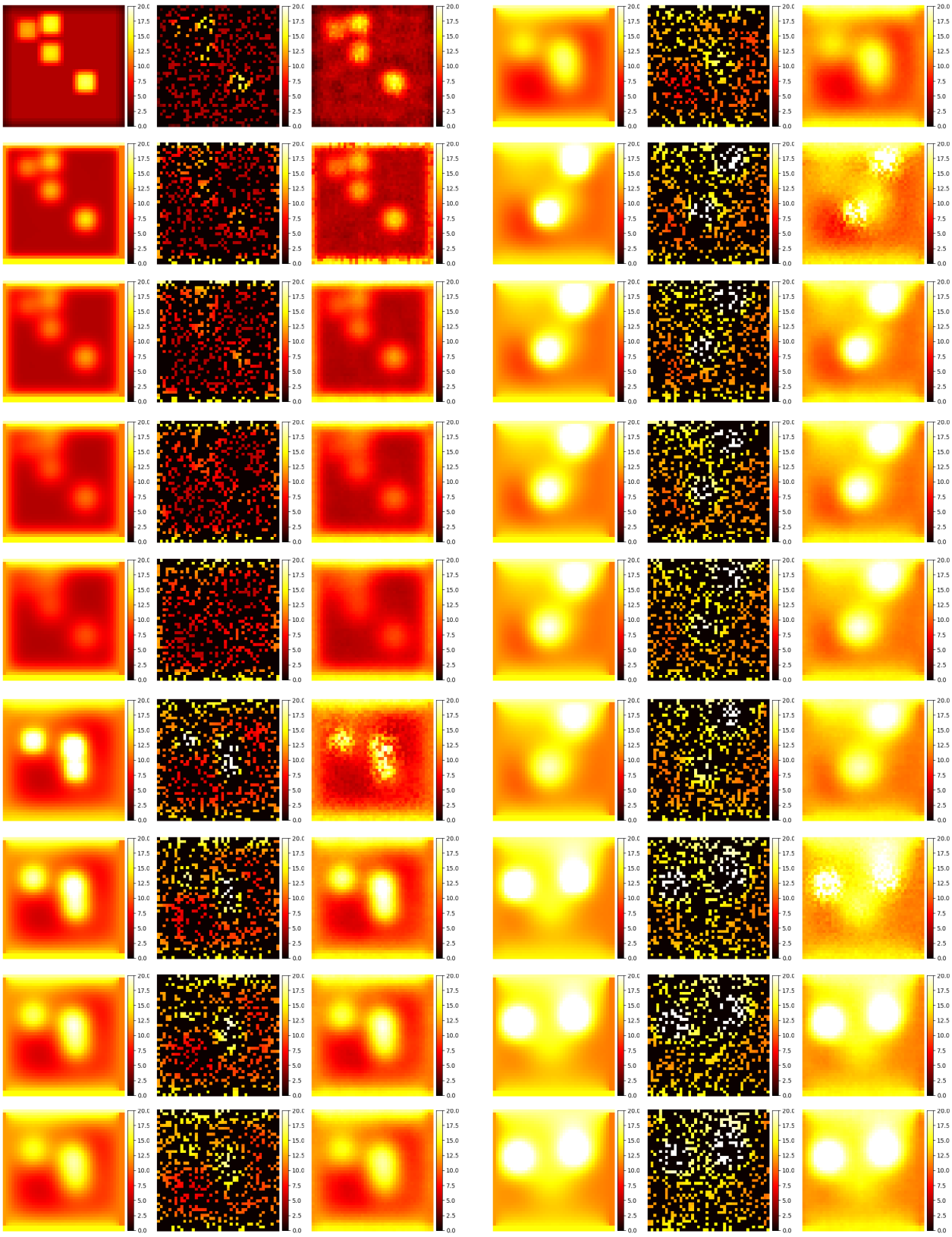

Fig. 8: Demonstration of compressive sensing reconstruction: For the first three columns, from left to right are original, sensed, and estimated fields, respectively. Similarly for last three columns. In the first three columns, from top to bottom rows are the frame number 1, 20, 40, 60, 80, 100, 120, 140, 160, respectively. Similarly, in last three columns are the frame number 180, 200, 220, 240, 260, 280, 300, 320, 340, respectively